Comparative phase transformation and magnetocaloric effect study of Co and Mn substitution by Cu in MnCoGe compounds

S. K. Pal[1*], C. Frommen[1], S. Kumar[2], B. C. Hauback[1], H. Fjellvåg[2], T. G. Woodcock[3], K. Nielsch[3], G. Helgesen[1#]

[1]Physics Department, Institute for Energy Technology (IFE), P.O. Box 40, 2027 Kjeller, Norway.
[2]Nanostructures and Functional Materials (NAFUMA), Department of Chemistry, University of Oslo, Sem Sælands vei 26, 0371 Oslo, Norway.

[3] IFW Dresden, Institute of Metallic Materials, Helmholtzstr. 20, 01069 Dresden, Germany

Corresponding author: *skpal099@gmail.com, #geir.helgesen@ife.no

ABSTRACT

Structural and magnetic phase transformations and magnetocaloric effect of Mn and Co substitutions by Cu in MnCoGe have been investigated using X-ray diffraction, differential scanning calorimetry, and magnetization measurements. Increase in Cu concentration reduces the martensitic structural and magnetic phase transition temperatures. However, nearly doubling of the amount of Co substitution is required compared to Mn for an equivalent change in the structural transition temperature. A giant magnetocaloric effect, $-\Delta S_M^{max} \approx 50$ $J.kg^{-1}K^{-1}$ for $\Delta\mu_0 H = 5$ T, resulting from coupling of concomitant structural and magnetic transformations near room temperature has been obtained for a sample with around 11 *at.%* Mn-substitution. Fine tuning of Cu concentration (20 *at.%*) in the case of Co substitution resulted in concurrent structural and magnetic transitions at around 260 *K*. However, the absence of a magnetostructural coupling resulted in peak entropy change of less than 4 $J.kg^{-1}K^{-1}$. Samples with 15 *at.%* or higher Co-substitution showed complex magnetic behavior and multiple magnetic transitions. The nature of magnetic phase transitions in both Co- and Mn-substituted samples have been investigated and phase diagrams for both set of samples have been derived based on calorimetry and magnetometry results.

Keywords

Magnetocaloric effect, Magnetic entropy, Magnetostructural coupling, Magnetic phase diagram, Martensitic transition, Mn-Co-Ge

1. Introduction

Recently, MM′X (M, M′ – transition metals and X – p-block elements) type compounds have attracted considerable research interest because of their magneto- and thermo-responsive properties[1,2]. In particular, magnetocaloric effect (MCE), a thermal response of a magnetic material upon application or removal of a magnetic field, is of significant importance for its potential application in environmental friendly and energy efficient magnetic cooling technology. Materials going through a first-order magnetic phase transition are known to produce the highest MCE; as such systems possess different crystal structures on either side of the magnetic transition and exhibit a large magnetization difference around the transition temperature. Equiatomic MnCoGe is an important member of MM'X family with both structural and magnetic phase transformations. The martensitic structural transition is reported to take place from high temperature Ni_2In-type hexagonal ($P6_3/mmc$, #194) austenite to low temperature TiNiSi-type orthorhombic (Pnma, #62) martensite at around 500 *K*, and both hexagonal and orthorhombic structures order ferromagnetically at Curie temperatures (T_C) of 275 and 355 *K*, respectively [3–5]. Additionally, saturation magnetization of the martensitic phase ($M_s = 3.86$ $\mu_B/f.u.$) is slightly higher as compared to that of the austenite phase ($M_s = 2.58$ $\mu_B/f.u.$), which is also indicative of a magnetic field-induced martensitic phase transition [6]. In pristine MnCoGe, the martensitic transformation takes place in the paramagnetic (PM) austenite state, but it is possible to reduce the martensitic transition temperature (T_{str}) to be close to the T_C of the martensitic phase. In such case, the material would transform from the low moment austenite to the high moment martensite phase, leading

to a large change in the magnetization accompanied by a first-order transition, which is basically the desired condition for a large change in the magnetic entropy and thus a giant MCE.

There have been some attempts in the past to reduce T_{str} of MnCoGe by applying physical pressure or inducing chemical pressure through elemental substitution and interstitial doping or vacancies [7–14]. The T_{str} is reported to decrease with both physical and chemical pressure. However, there are mixed opinions regarding the exact cause for decrease in the T_{str}. Although, there are significant differences in atomic bonding in these structures – the high-temperature phase is stabilized by one additional Mn-Ge, one Co-Ge and two Mn-Mn bonds; whereas, the low-temperature form has two additional short Co-Co interactions per formula unit (*f.u.*) [3]. However, these differences do not explain the stability of one phase over other. Moreover, some parameters like valence electron concentration (VEC), electronegativity, *c/a* ratio and Mn-Mn separation have been suggested as probable explanations for decrease of T_{str} [15–19]. Nonetheless, the mechanism and the factors leading to martensitic transition are not yet fully understood. Magnetic transition is also sensitive to interatomic distances and bond angles. Gercsi *et al.* [20] have shown that by tuning the Mn-Mn separation different magnetic orders (ferromagnetic and antiferromagnetic) can be stabilized in $MnCoGe_{1-x}P_x$ compounds. Hence, elemental substitution in MnCoGe can be used for tuning both the structural and the magnetic transitions. Mn and/or Co have been substituted by a series of elements such as Fe, Ni, V, Ti, Zn, Cu, Cr, Nb in order to tune T_{str} and T_C [8–10,18,21,22]. Li *et al.* [8] have performed a study of both Mn and Co substitution by Fe, and in spite of different chemical and physical properties of these two atoms, both magnetic and structural properties of the compounds were comparable. Ren *et al.* [23] have reported that a 4 *at.%* substitution of Fe for Co in MnCoGe is sufficient to tune the magnetostructural transition at 299 *K*, leading to maximum magnetic entropy change ($-\Delta S_M$) of 11 $J.kg^{-1}K^{-1}$ for a magnetic field change (ΔH) = 5 *T*. Aryal *et al.* [24] obtained a first-order magnetostructural transition in $Mn_{1-x}Al_xCoGe$ in range $0 \leq x \leq 0.01$ with a maximum ($-\Delta S_M$) of 12 $J.kg^{-1}K^{-1}$ for $\Delta H = 5$ *T* at 286 *K*. However, for $0.01 < x \leq 0.02$, the structural transition was below the magnetic transition and hence no magnetostructural coupling could be established. Gao *et al.* [25] investigated the effect of Ge substitution by In in MnCoGe and reported that a small amount of In (2 *at%*) can shift the magnetostructural transition to room temperature which produced maximum ($-\Delta S_M$) value of 25.4 $J.kg^{-1}K^{-1}$ for $\Delta H = 5$ *T*. In addition to large magnetocaloric effect, the substitution of In for Ge in MnCoGe also shows a giant barocaloric effect. Wu *et al.* [26] have reported a very large magnetic entropy change of 52 $J.kg^{-1}K^{-1}$ at around 300 *K* in $MnCoGe_{0.99}In_{0.01}$ under an applied hydrostatic pressure of only 3 *kbar*, this value of magnetic entropy change exceeds that of the most materials including LaFeSi under 5 *T* of magnetic field change. Here, we have carried out substitutions of Mn and Co atoms by non-magnetic Cu and performed a detailed study of their magnetic and structural properties in order to gain a better understanding and the significance of these two individual positions.

2. Experimental.

Polycrystalline ingots of $MnCo_{1-x}Cu_xGe$ ($x = 0$-0.25) and $Mn_{1-x}Cu_xCoGe$ ($x = 0$-0.15) were prepared by arc-melting of metal elements Mn, Co, Cu, Ge of purity 99.99% or higher in a water-cooled copper crucible under argon gas atmosphere. These arc-melted ingots were then wrapped in Ta foil, sealed in evacuated quartz ampoules and homogenized by heat treating under partial vacuum at 1123 *K* for 100 hours and then furnace-cooled to room temperature (RT). X-ray diffraction (XRD) measurements were performed at RT on powder samples using a Bruker D8 Advance diffractometer operating in reflection mode with Cu-K_α radiation for structural characterization of various samples. Phase matching and unit cell refinements were carried out using the FullProf/WinPLOTR suite [27]. The structural transformation was studied using differential scanning calorimetry (DSC 25 – TA Instruments) with a heating/cooling rate of 5 *K/min*. A superconducting quantum interface device (SQUID – Quantum Design MPMS 5S) and a physical property measurement system (Quantum Design - PPMS) were employed to measure isofield (M-T) and isotherm (M-H) magnetization curves. Samples for the magnetic measurements were prepared by mixing the fine-irregular-shaped powder particles with a non-

magnetic glue and incapsulating the mixture in gelatin capsules. The glue was used to prevent any rotation of the particles in magnetic field. The M-T measurement was performed at a temperature step at 2 *K* with a heating or cooling rate of 2 *K/min.*, adopting the settle mode for setting of the temperature. In case of M-H measurement, the magnetic field was set in persisting mode which provides a stable field. The field was changed at intervals of 0.02 and 0.2 *T* in 0-1 *T* and 1-5 *T* ranges, respectively. The magnetization curves were not corrected for demagnetizing field due to the irregular shape of the sample and the powder particles. The magnetocaloric effect was evaluated from the M-H curves following the loop method (refer to [28,29] for more details) using the integral form of the Maxwell's relation. In the loop process when measuring isotherms in the cooling run, the sample is always heated to a fixed temperature in paramagnetic state after each isotherm measurement and then cooled down to the desired measuring temperature. This process erases the history of the sample and the magnetic response doesn't get affected by the coexistence of the mixed para- and ferro-magnetic phases [28].

3. Results and discussion

Fig. 1(a) and 1(b) show RT powder XRD patterns of $MnCo_{1-x}Cu_xGe$ and $Mn_{1-x}Cu_xCoGe$ compounds, respectively. It is evident from these data that the crystal structure changes from TiNiSi-type orthorhombic (Pnma #62) to Ni_2In-type hexagonal ($P6_3/mmc$ #194) with the substitution of Co and Mn by Cu. This suggests that in both cases, Cu substitution plays a crucial role in altering the phase stability. Additionally, the martensitic transformation temperature can be lowered from higher temperature to temperatures well below RT by such a substitution. Coexistence of orthorhombic and hexagonal phases at RT can be seen for x = 0.18 and x = 0.10 for Co and Mn substitutions, respectively, indicating that structural transformation for these compounds takes place near RT. Lattice constants and unit cell volumes obtained from profile fitting of the XRD patterns and unit cell refinements using the WinPLOTR/FullProf suite are shown in Fig. 2. Lattice constants *a*, *b* and *c* behave differently with the Cu substitution. In case of Mn substitution by Cu, *a* and *b* decrease while *c* slightly increases for orthorhombic phase, whereas, both *a* and *c* decrease for hexagonal phase with increasing Cu concentration. On the other hand, increasing Cu substitution for Co results in an increase of *a* and *c*, and a decrease of *b* for orthorhombic phase, while, both *a* and *c* show a minute increase for hexagonal phase. The unit cell volume (*V*), for both orthorhombic and hexagonal phases decreases with increasing Cu substitution for Mn, whereas, an increase in *V* can be seen for Co substitution. It is interesting to note that *V* of hexagonal phase for Co substitution shows only a minuscule increase. This change in unit cell volume may be attributed to differences in atomic sizes of the said elements. As radius of Cu (~1.28 Å) atom is smaller than that for Mn (~1.30 Å) atom while larger than that for Co (~1.25 Å) atom [30, 31], a substitution of Cu for Mn and Co would lead to lattice contraction and expansion, respectively. According to unit cell volume relationship ($V_{ortho} = 2V_{hex}$) of orthorhombic and hexagonal structures [3], unit cell volume increase (($V_{ortho} - 2V_{hex}$)/$2V_{hex}$) of 3.9% and 4.1% for Mn and Co substitutions, respectively, were obtained due to the martensitic transformation from hexagonal to orthorhombic structure at RT. These large values for unit cell volume change reveal a significant volume expansion resulting in a large degree of lattice distortion during the martensitic transformation. Overall effect of atomic size differences between Cu-Mn and Cu-Co are evident in the lattice volume for both orthorhombic and hexagonal phases. Lattice volume change is mainly a result of change in the cell parameter *a*, as the percentage change in orthorhombic cell parameters *b* and *c* is only around 0.2 %, whereas, for *a* its around 1 %. This asymmetric change in unit cell can be a result of atomic arrangement in orthorhombic structure that is a distortion of ordered hexagonal structure.

Fig. 3(a)-3(c) show DSC heat-flow curves along with M-T curves for Co- and Mn-substituted samples. DSC curves reveal that T_{str} for both the Co- and Mn-substituted samples decrease continuously with increasing Cu concentration. Variation of T_{str} with respect to x for Co- and Mn-substituted samples is shown in Fig. 3(d). Upper curves in shaded patterns represent onset and lower ones the end-set of the martensitic transition during cooling process. It is evident from width of shaded regions that Mn-substituted samples show a faster martensitic transition compared to that of Co-substituted samples.

Additionally, T_{str} decreases much faster with Mn substitution compared to that of Co substitution. Moreover, roughly a doubling of amount of Co-substitution compared to that of Mn is required to produce a similar change in T_{str}.

Phase transition in MnCoGe occurs *via* diffusionless atomic displacements and all atoms show changes in their coordination during this transition. Low-temperature phase can be described as an orthorhombic distortion of hexagonal phase. As reported by Jeitschko *et al.* [3], there are significant differences in interatomic distances and bonding of Mn-Ge, Co-Ge, Co-Co and Mn-Mn atoms between orthorhombic and hexagonal phases. However, no satisfactory explanation regarding structure stabilization can be determined from these differences in bonding. Furthermore, as orthorhombic structure is considered as a distortion of hexagonal one, an increase of *c/a* ratio of the orthorhombic structure with increasing Cu concentration suggest that Cu substitution would lead to stabilization of hexagonal structure at a lower temperature. The *c/a* ratio of Mn-substituted samples increases from 1.183 to 1.189 for an increase of Cu concentration from 0 to 10 *at.%*, which clearly supports the above argument of decreasing T_{str} with decreasing *c/a* ratio (or increasing Cu concentration). However, the *c/a* ratio was found to decrease from 1.183 to 1.173 for an increase of Cu concentration from 0 to 15 *at.%*, in the case of Co substitution. This decrease in *c/a* ratio is basically attributed to increase in *a*, possibly due to the larger atomic size of Cu compared to that of Co, and also due to an enhanced distortion in the orthorhombic *a-b* plane.

The valence electron concentration (VEC) [32], determined as the concentration-weighted sum of outer shell s, p and d electrons, has been proposed to significantly affect the structural transition [33,34]. As the VEC for Cu (VEC = 11 is higher than that of both Mn (VEC = 7) and Co (VEC = 9), an increase in Cu concentration would lead to an increase of total VEC in both these cases. VEC for $MnCo_{1-x}Cu_xGe$ was calculated as the weighted sum of all the elements using formula VEC ($MnCo_{1-x}Cu_xGe$) = 1 * VEC (Mn) + (1-x) * VEC (Co) + x * VEC (Cu) + 1 * VEC (Ge) and in similar way for $Mn_{1-x}Cu_xCoGe$. It is evident from Fig. 3(d) that T_{str} decreases with the VEC. It is important to note that T_{str} is nearly constant up to VEC = 10.07 corresponding to around 9 *at.%* of Cu for both Co and Mn substitutions. Beyond VEC = 10.07, T_{str} for Co-substituted samples decreases at a faster rate compared to that of Mn-substituted samples. The dependence of T_{str} on the VEC has also been reported on similar MnCoGe systems by creating Mn or Co vacancies, and substitution of Co by Mn, and Ge by Al or Ga atoms [34-38]. It is important to point out that these vacancies and substitution lead only to a decrease in the VEC. On the contrary, present study where the VEC increases with substitution shows a reverse behavior as T_{str} decreases with increasing the VEC. Similar behavior has also been observed in case of the Zn (VEC = 12) substitution for Mn and Co atoms in MnCoGe compounds [18,39]; where T_{str} decreases with increasing VEC of $Mn_{1-x}Zn_xCoGe$ and $MnCo_{1-x}Zn_xGe$ compounds. Thus, from these observations, it becomes ambiguous to say whether the T_{str} varies positively or negatively with the VEC. The reduction of the T_{str} may also be accounted for in terms of the difference in electronegativity of Cu and Mn/Co. Substitution of a more-electronegative element Cu (χ_{Cu}=1.90) at Mn (χ_{Mn}=1.55) or Co (χ_{Co}=1.65) site is expected to lead to stronger bonds and thus resulting in the reduction in T_{str} [15,39]. Faster decrease in T_{str}, for of Mn substitution, as compared to that of Co one is in accordance with larger difference in electronegativity of Cu and Mn as compared to that of the Cu and Co.

Temperature dependent magnetization (M-T) curves for Co- and Mn-substituted samples measured in presence of magnetic field, $\mu_0 H = 0.1$ *T* are presented in Fig. 3(a)-3(c). The M-T curves of the Co-substituted samples ($x \leq 0.15$) show almost no hysteresis and thus reveal second-order nature of the ferromagnetic (FM) transition (Fig. 3(a)). In addition, T_C is rapidly reduced from 355 *K* for x = 0 to 265 *K* for x = 0.15. Note that these magnetic transitions for x = 0-0.15 samples belong to the orthorhombic phase. Interestingly, the $x \geq 0.15$ samples show a complex magnetic behavior with a dip in the M-T curve at lower temperatures, *e.g.*, around 125 *K* for x = 0.15 and around 175 *K* for x = 0.19 and 0.20. Possible causes for such a dip in M-T curves could be due to presence of antiferromagnetic interaction or spin-reorientation. The presence of several magnetic sub-lattices with different thermal behavior can also result in such a dip. The determination of the exact physical origin behind this dip is a subject of

further detailed investigation. In addition, M-T curves show multiple magnetic transitions. The almost unchanged T_C for the hexagonal phase (for x = 0.19-0.25) can be attributed to magnetic exchange interactions that are not substantially affected by an increase in Cu-concentration as lattice parameters *a* and *c* remain almost unchanged with increasing x value (see Fig. 2). As evident from Fig. 3(a), T_C of x = 0.19 and 0.20 samples coincide with T_{str}. Presence of multiple magnetic transitions can be seen in the enlarged M-T curve of the x = 0.19 sample shown as inset of Fig. 3(a). The transition around 260 *K* showing an increase of magnetization with decreasing temperature corresponds to the Curie temperature, T_{C1} of the hexagonal phase. Slope of M-T curve changes with a reduced rate of increase in the magnetization around 250 *K*. This can be attributed to structural transition that takes place from a FM-hexagonal to a PM-orthorhombic structure. During this transformation, fraction of FM phase decreases with temperature and hence its contribution to magnetization is expected to decrease. Furthermore, as the temperature approaches the Curie point, T_{C2} of the orthorhombic phase, magnetization increases again. This can be seen in terms of a slight change in the slope of the M-T curve at T_{C2}. The complex behavior at T_{m1} and T_{m2} is not fully understood yet, however, possible reasons may include antiferromagnetic interaction, spin reorientation transition or presence of different magnetic sublattices. Similar magnetic transitions are also visible in other samples with higher Cu concentrations. Moreover, as it is evident from M-T curves for $x \geq 0.19$ samples, that the zero-field-cooled, ZFC (solid-symbols, measured in the warming process) and the field-cooled, FCC (hollow-symbols, measured in the cooling process) magnetization curves split at temperatures below 270 *K*. Application of magnetic field is expected to favor ferromagnetic order, consequently, for higher fields the ordering temperature is increased resulting in shift of FCC curve towards higher temperature.

In contrast to Co case, substitution of Mn by Cu leads to a hysteretic and sharp, first-order magnetic transition for x = 0.09-0.12 (see Fig. 3(c)). This first-order transition may be attributed to the coupling of the magnetic and structural transitions occurring at nearly the same temperatures. A slightly broader magnetic transition and reduced thermal hysteresis in case of the x = 0.12 sample are ascribed to wider separation between T_C and T_{str}, while a de-coupling of the magnetic and structural transitions can be seen for samples x = 0.13 and 0.15. Non-hysteretic transition around 250 *K* and hysteretic transition near 175 *K* correspond to the second-order magnetic and first-order structural transitions, respectively.

M-H curves of selected Co- and Mn-substituted samples measured at various discrete temperatures are shown in Fig. 4(a) and 4(b). The Co-substituted samples show a typical second-order type ferromagnetic transition from PM to FM. However, the Mn-substituted sample shows a metamagnetic behavior and a first-order transition (Fig. 4(b)). Linear behavior of M-H curves at 300 *K* (Fig. 4(a)) and 310 K, 306 *K* (Fig. 4(b)), represents PM region. A sudden change in slope of the 304-300 *K* curves (see Fig. 4(b)) indicates a magnetic field induced transition from the PM-hexagonal to the FM-orthorhombic phase.

Fig. 5 represents negative magnetic entropy changes, $-\Delta S_M$ of Co- and Mn-substituted samples estimated from isothermal magnetization curves by using an integral form of Maxwell's relation, $\Delta S_M(T, \mu_0 H) = \int_0^{\mu_0 H} \left(\frac{\partial M(T,\mu_0 H)}{\partial T}\right)_H d(\mu_0 H)$. The broad $-\Delta S_M$ peaks for Co-substituted samples (Fig. 5(a)) are attributed to second-order nature of the magnetic transition. Two adjacent $-\Delta S_M$ peaks at around 225 and 270 *K* for x = 0.20 sample correspond to magnetic transition of hexagonal phase and first-order structural transition, respectively, as can be seen in Fig. 3(a). Although, structural and magnetic transition for the x = 0.20 sample are sufficient close enough, a contribution from a possible magnetostructural coupling cannot be seen in the $-\Delta S_M$ curves. In contrast to small and wide $-\Delta S_M$ peaks for Co-substituted samples, Mn-substituted samples show significantly large values of $-\Delta S_M$. The very large $-\Delta S_M$ values for x = 0.10 and 0.11 Mn-substituted samples (Fig. 5(b)) are basically attributed due to strong magnetostructural coupling where the PM-hexagonal phase transforms directly to the FM-orthorhombic phase leading to a sharp first-order magnetic phase transition. A partial coupling of the magnetic and structural transitions for x = 0.12, in which case the magnetic and structural transition temperature are not exactly overlapping, results in a $-\Delta S_M$ peak value of only 15 $J,Kg^{-1}K^{-1}$. Significantly reduced $-\Delta S_M$ value in case of x = 0.13 Mn-substituted sample (Fig. 5(c)) can be an effect of de-coupling of structural and magnetic

Table 1: Magnetic entropy change ($|\Delta S_M|_{max}$) corresponding to $\mu_0|\Delta H|$ field change, magnetic transition temperature (T_C) or magnetostructural transition temperature (T_{mst}) for selected magnetocaloric materials showing a transition around room temperature.

Materials	T_C/T^*_{mst} (K)	$\|\Delta S_M\|_{max}$ ($J.kg^{-1}.K^{-1}$)	$\mu_0\|\Delta H\|$ (T)	Ref.
Gd	294	11	5	40
$MnFeP_{0.45}As_{0.55}$	308	18	5	41
$LaFe_{11.57}Si_{1.43}H_{1.3}$	291	28	5	42
$MnCoGeB_{0.01}$	304*	14.6	5	13
$Mn_{0.89}Cr_{0.11}CoGe$	292*	27.7	5	43
$Mn_{0.965}CoGe$	292*	26	5	7
$Mn_{0.8}Zn_{0.2}CoGe$	300	3.5	1	18
$MnCo_{0.7}Zn_{0.3}Ge$	300*	12	5	39
$MnCo_{0.85}Cu_{0.15}Ge$	255	3.2	5	This work
$Mn_{0.90}Cu_{0.10}CoGe$	302*	40	5	This work
$Mn_{0.89}Cu_{0.11}CoGe$	255*	48	5	This work

* Represents the magnetostructural phase transition temperature in which case the magnetic transition is controlled by the structural transition.

transitions. The two peaks at around 240 and 160 *K* may be ascribed to magnetic and structural transitions, respectively. A comparison of the maximum entropy change values obtained in this work with some selected magnetocaloric compounds is presented in Table 1. It is evident that the Mn-substituted MnCoGe compound studied in this work shows significantly high magnetic entropy change near room temperature.

Concentration dependent phase diagrams of Co- and Mn-substituted samples based on calorimetry and magnetometry measurements during cooling process are presented in Fig. 6. It is evident that the structural transition temperature follows almost similar trend in both Co- and Mn-substituted samples, while magnetic transition temperatures differ significantly. T_C for both the orthorhombic and hexagonal phases in case of the Mn-substituted samples are almost Cu-concentration independent (see Fig. 6(b)). Additionally, T_C is controlled by T_{str} in the temperature range T_C (ortho) $\leq T \leq T_C$ (hex). This provides a wide temperature window for magnetostructural coupling leading to a giant MCE. On the other hand, in case of the Co-substituted samples T_C of orthorhombic phase decreases continuously with increasing Cu concentration, even T_C (ortho) tends to be lower than T_C (hex) for higher Cu concentrations ($x \geq 0.19$). This leads to the presence of several magnetic transitions at or below ~ 250 *K* for $x \geq 0.19$ samples. Furthermore, as T_C for orthorhombic phase becomes smaller than that of hexagonal phase, there is no direct transition from PM-hexagonal phase to FM-orthorhombic phase in these samples. Thus, first-order magnetostructural transition and hence giant MCE is not realized in case of Co-substituted samples.

4. Conclusions

A comparative study of structural and magnetic phase transformations and magneto-response properties of $MnCo_{1-x}Cu_xGe$ and $Mn_{1-x}Cu_xCoGe$ compounds has been performed in this work. The structural transition temperature for both Co- and Mn-substituted samples can be tuned far below the magnetic transition temperature. In addition, Mn substitution affects T_{str} more effectively compared to that of Co substitution. It is clear that due to differences in atomic radii, Cu substitution for Co and Mn results in chemical pressure which in turn alters T_{str}. However, exact reason for drop in T_{str} is not understood yet, it could be a combined effect of VEC, electronegativity, interatomic distances and magnetic interactions. Magnetic transition temperatures of orthorhombic and hexagonal phases for the case of Mn substitution are almost unaffected which leads to a wide temperature window for magnetostructural coupling resulting in a giant MCE with a maximum magnetic entropy change of around 50 $J.kg^{-1}.K^{-1}$ for a field change of 5 *T*. On the other hand, Co substitution by Cu results in a continuous decrease of T_C of orthorhombic phase which is likely due to weakening of Mn-Co or Co-Co magnetic interactions. This leads to multi magnetic phase transitions: PM-hex => FM-hex => PM-ortho => FM-ortho (for the

optimal x = 0.20 composition), instead of the desired direct PM-hex – FM-ortho first-order magnetostructural phase transition, and therefore Co-substituted samples show small < 3.5 $J.kg^{-1}.K^{-1}$ entropy change values.

Acknowledgements

This work was financially supported by the internal grants of Institute for Energy Technology (IFE), Norway. I am thankful to Prof. A. T. Skjeltorp for fruitful discussions and M. H. Sørby, K. Nenkov for their assistance with measurements and device operation.

References

[1] V. Johnson, Diffusionless orthorhombic to hexagonal transitions in ternary silicides and germanides, *Inorg. Chem.* 14 (1975) 1117-1120.

[2] J. H. Chen, Z. Y. Wei, E. K. Liu, X. Qi, W. H. Wang and G. H. Wu, Structural and magnetic properties of $MnCo_{1-x}Fe_xSi$ alloys, *J. Magn. Magn. Mater.* 387 (2015) 159-164.

[3] W. Jeitschko, A high-temperature X-ray study of displacive phase transition in MnCoGe, *Acta Cryst.* B31 (1975) 1187-1190.

[4] T. Kanomata, H. Ishigaki, T. Suzuki, H. Yoshida, S. Abe and T. Kaneko, Magneto-volume effect of $MnCo_{1-x}Ge_{(0\leq x\geq 0.2)}$, *J. Magn. Magn. Mater.* 140–144 (1995) 131-132.

[5] S. Lin, O. Tegus, E. Brück, W. Dagula, T. J. Gortenmulder and K. H. J. Buschow, Structural and magnetic properties of $MnFe_{1-x}Co_xGe$ compounds, *IEEE Trans. Magn.* 42 (2006) 3776-78.

[6] S. Kaprzyk and S. Niziol, The electronic struchyre of comnge with the hexagonal and orthorhombic crystal structure, *J. Magn. Magn. Mater.* 87 (1990) 267-75.

[7] E. K. Liu, W. Zhu, L. Feng, J. L. Chen, W. H. Wang, G. H. Wu, H. Y. Liu, F. B. Meng, H. Z. Luo and Y. X. Li, Vacancy-tuned paramagnetic/ferromagnetic martensitic transformation in Mn-poor $Mn_{1-x}CoGe$ alloys, *Euro phys. Lett.* 91 (2010) 17003-8.

[8] G. J. Li, E. K. Liu, H. G. Zhang, Y. J. Zhang, J. L. Chen, W. H. Wang, H. W. Zhang, G. H. Wu and S. Y. Yu, Phase diagram, ferromagnetic martensitic transformation and magnetoresponsive properties of Fe-doped MnCoGe alloys, *J. Magn. Magn. Mater.* 332 (2013) 146-59.

[9] C. L. Zhang, H. F. Shi, E. J. Ye, Y. G. Nie, Z. .D Han and D. H. Wang, Magnetostructural transition and magnetocaloric effect in MnCoGe-NiCoGe system, *J. Alloys Compd.* 639 (2015) 36-39.

[10] X. Si, Y. Liu, Y. Shen, W. Yu, X. Ma, Z. Zhang, Y. Xu, T. Gao, Critical behavior and magnetocaloric effect near room temperature in $MnCo_{1-x}Ti_xGe$ alloys, *Intermetallics* 93 (2018) 30–39.

[11] S. Y. Emre, The effect of Cr doping on the magnetic and magnetocaloric properties of MnCoGe alloys, *J. Magn.* 18 (2013) 405-11.

[12] D. Zhang, Z. Nie, Z. Wang, L. Huang, Q. Zhang and Y. D. Wang, Giant magnetocaloric effect in MnCoGe with minimal Ga substitution, *J. Magn. Magn. Mater.* 387 (2015) 107-10.

[13] N. T. Trung, L. Zhang, L. Caron, K. H. J. Buschow and E. Brück, Giant magnetocaloric effects by tailoring the phase transitions, *Appl. Phys. Lett.* 96 (2010) 172504-7.

[14] P. Shamba, J. L. Wang, J. C. Debnath, S. J. Kennedy, R. Zeng, M. F. M. Din, F. Hong, Z. X. Cheng, A. J. Studer and X. C. Dou, The magnetocaloric effect and critical behaviour of the Mn0.94Ti0.06CoGe alloy, *J. Phys.: Condens. Matter* 25 (2013) 56001-8.

[15] E. Liu, W. Wang, L. Feng, W. Zhu, G. Li, J. Chen, H. Zhang, G. Wu, C. Jiang, H. Xu and F. de Boer, Stable magnetostructural coupling with tunable magnetoresponsive effects in hexagonal ferromagnets, *Nat. Commun.* 3 (2012) 873-83.

[16] A. Quetz, T. Samanta, I. Dubenko, M. J. Kangas, J. Y. Chan, S. Stadler and N. Ali, Phase diagram and magnetocaloric effects in aluminum doped MnNiGe alloys, *J. Appl. Phys.* 114 (2013) 153909-14.

[17] T. Samanta, I. Dubenko, A. Quetz, S. Stadler and N. Ali, Large magnetocaloric effects due to the coincidence of martensitic transformation with magnetic changes below the second-order magnetic phase transition in $Mn_{1-x}Fe_xCoGe$, *J. Magn. Magn. Mater.* 330 (2013) 88.

[18] S. Cheng-Juan, L. Qiang, G. Yuan-Yuan, W. Dun-Hui and D. You-Wei, Magnetic phase transition and magnetocaloric effect in $Mn_{1-x}Zn_xCoGe$ alloys, *Chinese Phys. B* 23 (2014) 97502-6.

[19] C. L. Zhang, Z. D. Han, B. Qian, H. F. Shi, C. Zhu, T. Chen and T. Z. Wang, Magnetostructural transformation and magnetocaloric effect in $MnNiGe_{1-x}Ga_x$ alloys, *J. Appl. Phys.* 114 (2013) 153907-11.

[20] Z.Gercsi, K. Hono and K. G. Sandeman, Designed metamagnetism in $CoMnGe_{1-x}P_x$, *Phys. Rev. B* 83 (2011) 174403-6.

[21] X. Si, Y. Liu, Y. Shen, W. Yu, X. Ma, Z. Zhang, Y. Xu, T. Gao, Magnetocaloric effect in $Mn_{1-x}CoGeSi_x$ alloys, *J. Mater. Sci.* 53(5) (2018) 3661-3671.

[22] L. Caron, N. T. Trung and E. Brück, Pressure-tuned magnetocaloric effect in $Mn_{0.93}Cr_{0.07}CoGe$, *Phys. Rev. B* 84 (2011) 20414-8.

[23] Q. Y. Ren, W. D. Hutchison, J. L. Wang, A. J. Studer and S. J. Campbell, First-order magneto-structural transition and magnetocaloric effect in $Mn(Co_{0.96}Fe_{0.04})Ge$, *J. Alloys Compd.* 693 (2017) 32-39.

[24] A. Aryal, A. Quetz, S. Pandey, T. Samanta, I. Dubenko, M. Hill, D. Mazumdar, S. Stadler, N. Ali, Magnetostructural phase transitions and magnetocaloric effects in as-cast $Mn_{1-x}Al_xCoGe$ compounds, *J. Alloys Compd.* 709 (2017) 142-146.

[25] T. Gao, M. Wu, N. Qi, T. Zhou, X. Luo, Y. Liu, K. Xu, V. V. Marchenkov, H. Dong, Z. Chen, B. Chen, Giant low field magnetocaloric effect and magnetostructural coupling in $MnCoGe_{1-x}In_x$ around room temperature, *J. Alloys Compd.* 753 (2018) 149-154.

[26] R.-R. Wu, L.-F. Bao, F.-X. Hu, H. Wu, Q.-Z. Huang, J. Wang, X.-L. Dong, G.-N. Li, J.-R. Sun, F.-R. S., T.-Y. Z., X.-Q. Zheng, L.-C. Wang, Y. Liu, W.-L. Zuo, Y.-Y. Zhao, M. Zhang, X.-C. Wang, C.-Q. Jin, G.-H. Rao, X.-F. Han and B.-G. Shen, Giant barocaloric effect in hexagonal Ni2In-type Mn-Co-Ge-In compounds around room temperature, *Sci. Rep.* 5 (2015) 18027-37.

[27] T. Roisnel and J. Rodríquez-Carvajal, WinPLOTR: A Windows Tool for Powder Diffraction Pattern Analysis, *Mater. Sci. Forum* 378–381 (2001) 118-23.

[28] L. Caron, Z. Q. Ou, T. T. Nguyen, D. H. Cam Thanh, O. Tegus and E. Brück, On the determination of the magnetic entropy change in materials with first-order transitions, *J. Magn. Magn. Mater.* 321 (2009) 3559-66.

[29] G. F. Wang, Magnetic and calorimetric study of the magnetocaloric effect in intermetallics exhibiting first-order magnetostructural transitions, *Ph.D. thesis*, *Universidad de Zaragoza*, 2012.

[30] T. Samanta, I. Dubenko, A. Quetz, S. Stadler and N. Ali., Giant magnetocaloric effects near room temperature in $Mn_{1-x}Cu_xCoGe$, *Appl. Phys. Lett.* 101 (2012) 242405-8.

[31] T. Samanta, I. Dubenko,A. Quetz, S. Stadler and N. Ali, Large magnetocaloric effects over a wide temperature range in $MnCo_{1-x}Zn_xGe$, *J. Appl. Phys.* 113 (2013) 17A922-5.

[32] T. B. Massalski, Comments concerning some features of phase diagrams and phase transformations, *Mater. Trans.* 51 (2010) 583-96.

[33] T. Krenke, M. Acet, E. F. Wassermann, X. Moya, L. Mañosa and A. Planes, Ferromagnetism in the austenitic and martensitic states of NiMnIn alloys, *Phys. Rev. B* 73 (2006) 174413-23.

[34] S.-C. Ma, D.-H. Wang, H.-C. Xuan, L. -J. Shen, Q. -Q. Cao and Y. -W.Du, Effects of the Mn/Co ratio on the magnetic transition and magnetocaloric properties of $Mn_{1+x}Co_{1-x}Ge$ alloys *Chinese Phys. B* 20 (2011) 87502-6.

[35] L. F. Bao, F. X. Hu, R. R. Wu, J. Wang, L. Chen, J. R. Sun, B. G. Shen, L. Li, B. Zhang and X. X. Zhang, Evolution of magnetostructural transition and magnetocaloric effect with Al doping

in $MnCoGe_{1-x}Al_x$ compounds, *J. Phys. D. Appl. Phys.* 47 (2014) 55003-9.

[36] D. Zhang, Z. Nie, Z. Wang, L. Huang, Q. Zhang and Y. D. Wang, Giant magnetocaloric effect in MnCoGe with minimal Ga substitution, *J. Magn. Magn. Mater.* 387 (2015) 107-10.

[37] L. Caron, X. F. Miao, J. C. P. Klaasse, S. Gama and E. Brück, Tuning the giant inverse magnetocaloric effect in $Mn_{2-x}Cr_xSb$ compounds, *Appl. Phys. Lett.* 103 (2013) 112404-9.

[38] T. Samanta, I. Dubenko, A. Quetz, S. Temple, S. Stadler and N. Ali, Magnetostructural phase transitions and magnetocaloric effects in $MnNiGe_{1-x}Al_x$, *Appl. Phys. Lett.* 100 (2012) 052404-7.

[39] D. Choudhury, T. Suzuki, Y. Tokura and Y. Taguchi, Tuning structural instability toward enhanced magnetocaloric effect around room temperature in $MnCo_{1-x}Zn_xGe$, *Sci. Rep.* 4 (2014) 7544-50.

[40] S. Yu. Dan'kov, A. M. Tishin, V. K. Pecharsky, and K. A. Gschneidner, Magnetic phase transitions and the magnetothermal properties of gadolinium, *Phys. Phys. Rev. B* 57 (1998) 3478–3490.

[41] O. Tegus, E. Brück, K. H. J. Buschow and F. R. de Boer, Transition- metal-based magnetic refrigerants for room-temperature applications, *Nature* 415 (2002) 150-2.

[42] A. Fujita, S. Fujieda, Y. Hasegawa, and K. Fukamichi, Itinerant-electron metamagnetic transition and large magnetocaloric effects in $La(Fe_xSi_{1-x})_{13}$ compounds and their hydrides, *Phys. Rev. B* 67 (2003) 104416-28.

[43] N. T. Trung, V. Biharie, L. Zhang, L. Caron, K. H. J. Buschow, and E. Brück, From single- to double-first-order magnetic phase transition in magnetocaloric $Mn_{1-x}Cr_xCoGe$ compounds, *Appl. Phys. Lett.* 96 (2010) 162507-10.

Figures:

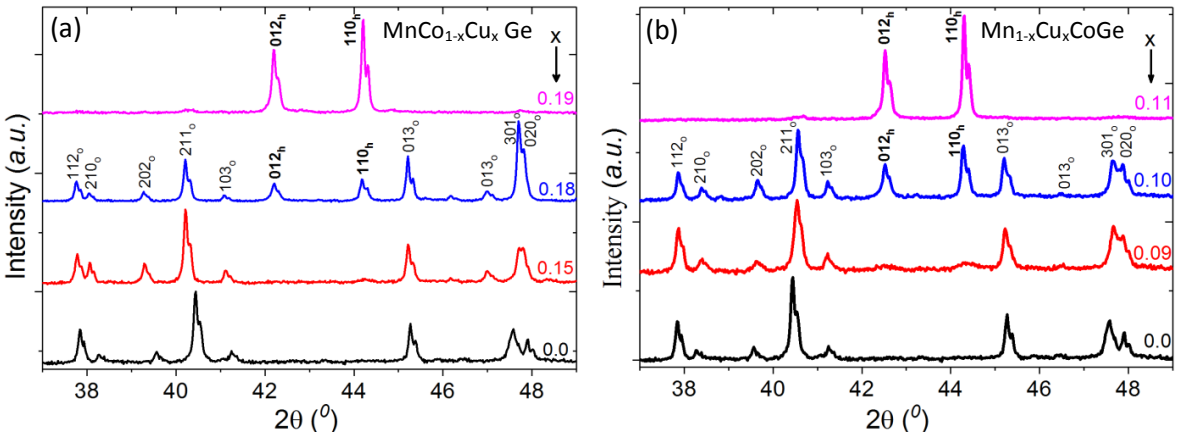

Fig. 1: XRD patterns of (a) $MnCo_{1-x}Cu_xGe$ (x = 0, 0.15 0.18, 0.19) and (b) $Mn_{1-x}Cu_xCoGe$ (x = 0, 0.09, 0.10, 0.11) measured at RT. The hkl_o and hkl_h denote the miller indices for the TiNiSi-type orthorhombic and the Ni_2In-type hexagonal structures, respectively.

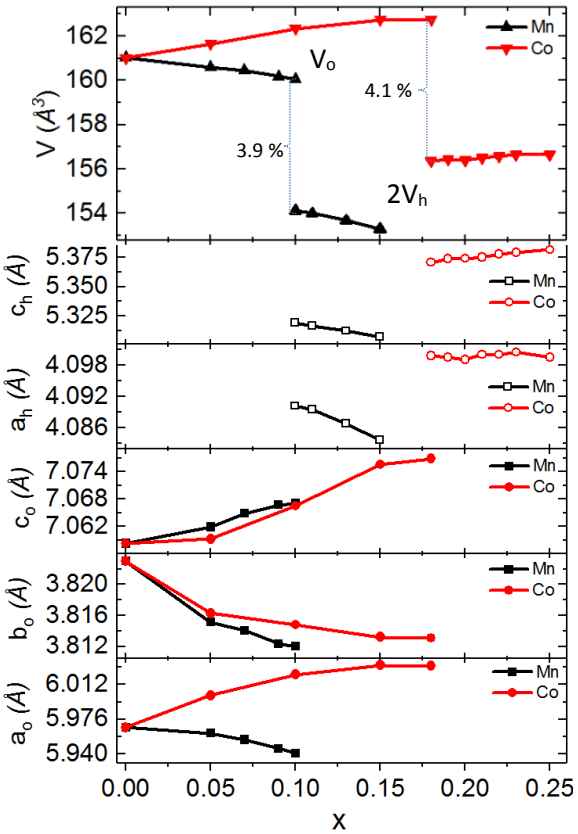

Fig. 2: Unit cell parameters for orthorhombic (a_o, b_o, c_o, V_o) and hexagonal (a_h, c_h, V_h) structures of $Mn_{1-x}Cu_xCoGe$ (legend-Mn) and $MnCo_{1-x}Cu_xGe$ (legend-Co) compounds. Error bars lie within the range of symbols.

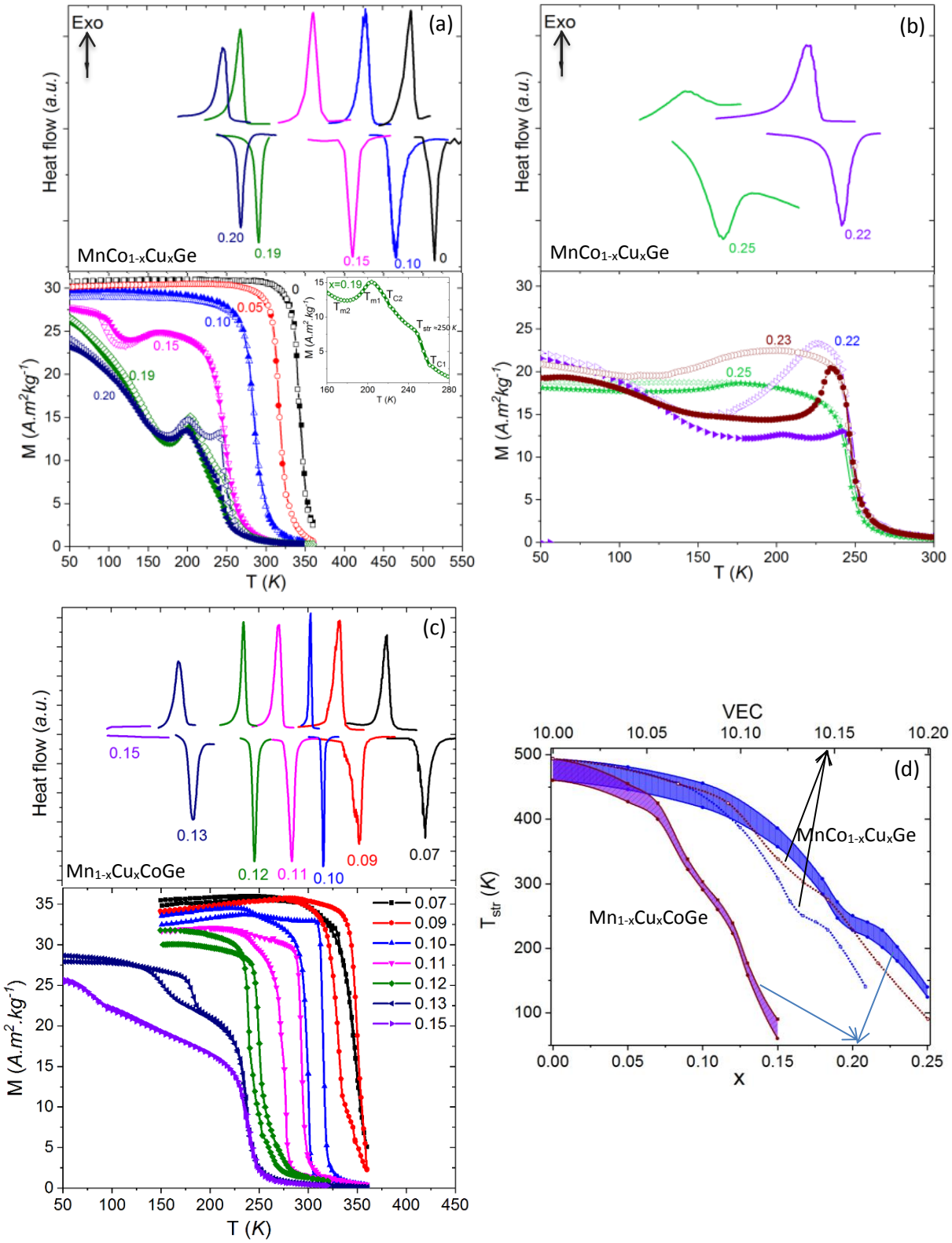

Fig. 3: DSC heat-flow and magnetization curves as a function of temperature for (a), (b) $MnCo_{1-x}Cu_xGe$ and (c) $Mn_{1-x}Cu_xCoGe$ compounds. The heat flow was measured at a heating/cooling rate of 5 K/min. whereas for the magnetization measurements were carried out at a heating/cooling rate of 2 K/min. Filled and hollow symbols correspond to zero-field cooled (ZFC) and field-cooled-cooling (FCC) magnetization measurements, respectively. (d) Structural transition temperature (T_{str}) as a function of Cu concentration x (solid curves) and valence electron concentration VEC (dotted curves) for $MnCo_{1-x}Cu_xGe$ and $Mn_{1-x}Cu_xCoGe$ compounds.

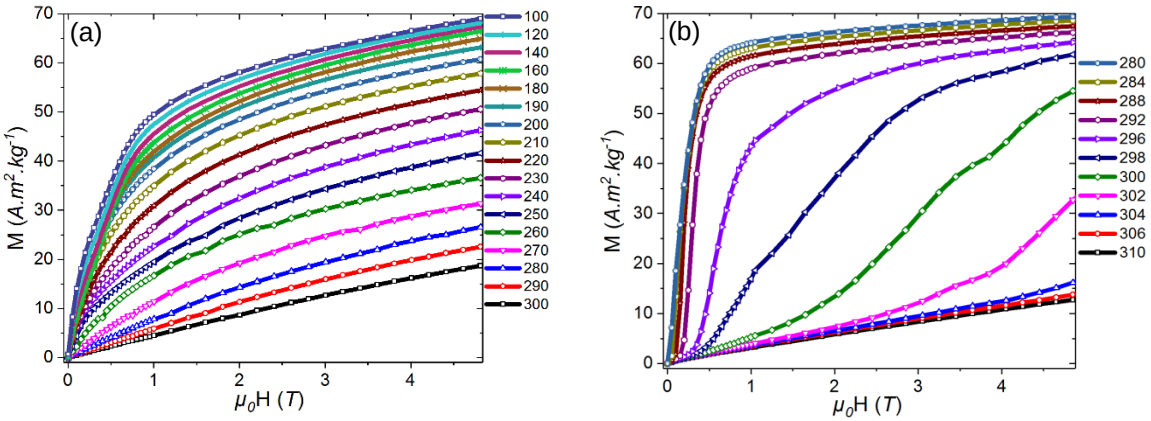

Fig. 4: (color online) Isothermal magnetization (M *vs* μ_0H) curves of (a) $MnCo_{0.80}Cu_{0.20}Ge$ and (b) $Mn_{0.90}Cu_{0.10}CoGe$.

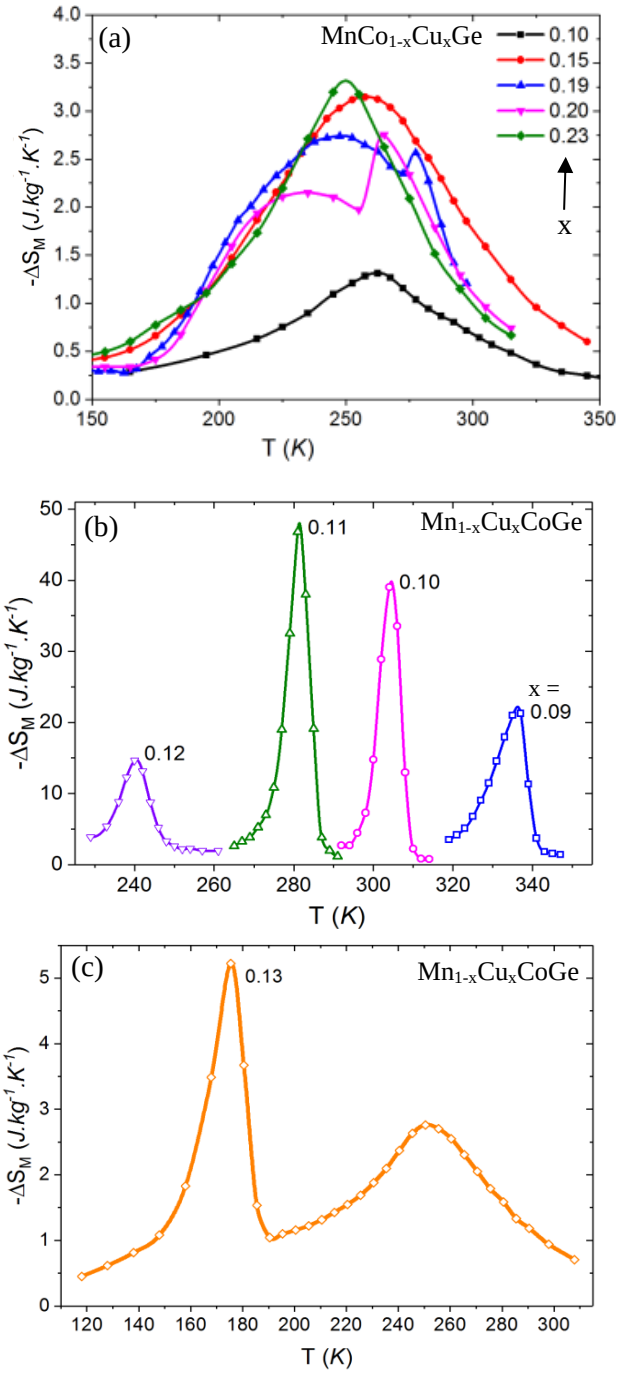

Fig. 5: (color online) Magnetic-entropy changes ($-\Delta S_M$) of (a) $MnCo_{1-x}Cu_xGe$ and (c)-(d) $Mn_{1-x}Cu_xCoGe$ for a field change of 5 *T* derived from isothermal magnetization curves. Note the scale differences in (b) and (c).

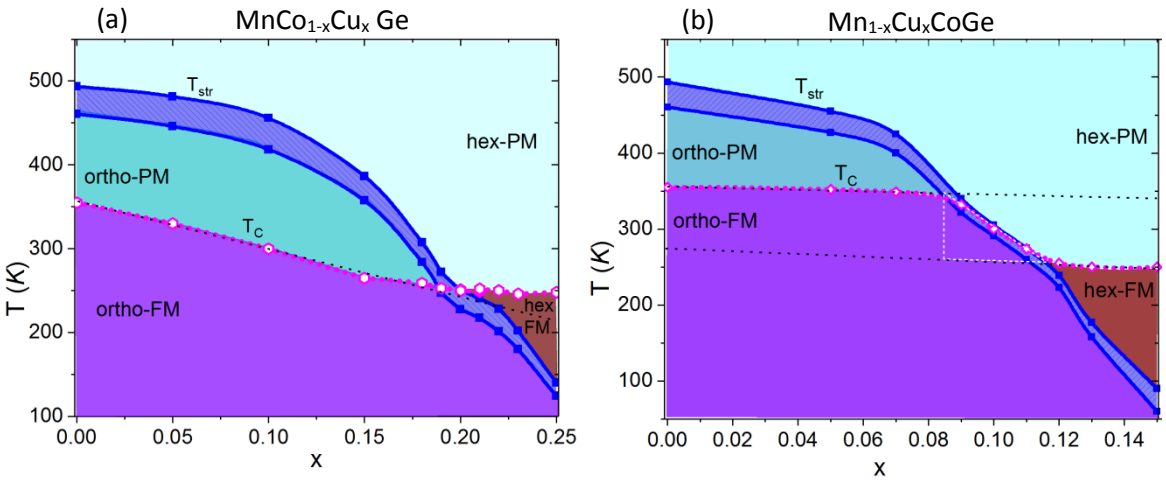

Fig. 6: (Colors online) Magnetic and structural phase diagrams of (a) $MnCo_{1-x}Cu_xGe$ and (b) $Mn_{1-x}Cu_xCoGe$ compounds based on results from magnetometry and calorimetry measurements. Upper and lower blue-curves with solid squares correspond to start and finish of the martensitic transformation temperature. Dotted-black lines represent a trend of T_C in entire composition range. Triangle with dashed-white lines in (b) represents interesting temperature and composition range for magnetostructural coupling.